2009

Microscopic Dynamics of the Orientation of a Hydrated Nanoparticle in an Electric Field

C. d. Daub

D. Bratko
Virginia Commonwealth University, dbratko@vcu.edu

A. Towshif

A. Luzar

Microscopic Dynamics of Hydrated Nanoparticle Orientation in an Electric Field

Christopher D. Daub,[1] Dusan Bratko,[1,2] Towshif Ali,[1] and Alenka Luzar[1,*]

[1]*Department of Chemistry, Virginia Commonwealth University, Richmond, Virginia USA, 23284*
[2]*Energy Biosciences Institute, University of California, Berkeley, California USA, 94720*

(Dated: September 16, 2009)

We use atomistic simulations to study the orientational dynamics of a nonpolar nanoparticle suspended in water and subject to an electric field. Due to molecular-level effects we describe, the torque exerted on the nanoparticle exceeds continuum-electrostatics based estimates by about a factor of two. The reorientation time of a $16.2\times16.2\times3.35$ Å^3 nanoparticle in a field $\mathbf{E} > 0.015$V/Å is an order of magnitude less than the field-free orientational time (~ 1 ns). Surprisingly, the alignment speed is nearly independent of the nanoparticle size in this regime. These findings are relevant for design of novel nanostructures and sensors and development of nanoengineering methods.

PACS numbers: 61.20.Ja, 68.08.De, 82.60.Qr

A particle with dielectric constant ϵ immersed in a medium with a different dielectric constant ϵ_m and subject to an external field tends to maximize the interfacial area which is parallel to the field direction. This fact can be exploited, for example, to estimate the magnitude and direction of electric fields by suspending a disc of known ϵ in the field and observing its motion [1]. The phenomenon has already been used in engineering processes at small length scales, including electrical control of optical properties [2], dielectrophoresis [3–6] and nanoassembly [6–10]. The key question of the *dynamics* of nanoparticle reorientation, however, cannot be addressed by conventional continuum theories for aligning forces [1, 2, 5, 8, 9], which become unreliable at the nanoscale. In this Letter, we determine the pertinent timescales by molecular simulation.

The prerequisite to solving this dynamic problem is the calculation of torques exerted on a hydrated nanopaticle in electric field. Such a calculation has so far not been presented. Our molecular study [11] of electrowetting behavior by a confined aqueous nanofilm [12, 13], however, suggests a notable augmentation of the alignment tendency in the field due the orientational bias [14, 15] of interfacial hydrogen bonds. This effect also depends on field *polarity*, in addition to its strength and direction. Acting in concert with the more general but polarity-insensitive tendency of all dipolar fluids [16] to arrange their dipoles parallel to both the interface as well as the applied field, a torque is exerted which tends to align the interface with the field. This contribution, arising from molecular asymmetry, is of the same order of magnitude as the torque due to the favorable head-tail arrangement of interfacial water dipoles [16, 17]. In the more interesting and practically relevant scenario of a nanoparticle immersed in the solvent, we therefore expect to observe a significant aligning torque even if $\epsilon \approx \epsilon_m$. Below we demonstrate that the aligning torque on a hydrated nanoparticle in electric field is significantly larger than continuum model predictions.

The *dynamics* of nanoparticle alignment [9], crucial for practical applications, is determined here for the first time. For nanoscale particles in water, we find that the response to the applied field is sufficiently fast (< 250 ps) that this mechanism is likely to be relevant in biological processes and could be exploited in the design of new sensor methods and synthesis of novel materials.

σ_{LJ}/Å	ϵ_{LJ}/kcal mol^{-1}	Inter-layer spacing/Å	Intra-layer spacing/Å
3.214	0.023	3.348	1.616

Label	n_{side}	n_{plane}	n_{total}	d_{side}/Å	n_w	b_{el}/Å	c_{el}/Å
S	8	64	128	11.31	892	7.30	2.25
M1	11	121	242	16.16	892	10.43	2.25
M2	11	121	242	16.16	1906	10.43	2.25
L	16	256	512	24.24	1762	15.65	2.25

TABLE I: Model parameters and dimensions of simulated smaller (S), medium (M), and larger (L) nanoparticle systems. n_{side}, n_{plane} and n_{total} are the number of atoms along each side, in each plane and in the entire nanoparticle, respectively. d_{side} is the length along one side, n_w the number of surrounding water molecules, and b_{el} and c_{el} are respectively the radii of the short and long axes when the nanoparticle is approximated as an ellipsoid for analytical calculations (see text).

We study the orientation of a nanoparticle immersed in water and under the influence of a static electric field using classical molecular dynamics (MD)[38]. The water is described using the SPC/E model [18] due to its good performance in reproducing dynamic properties. The nanoparticle is composed of two layers of carbon-like atoms, arranged in a simple rectangular lattice with the same surface/areal density as the hexagonal (111) face of graphene. The Lennard-Jones parameters and the lattice spacings of the atoms are given in Table I. The simulation box contained 892 water molecules, and a single nanoparticle of a given size, defined as in Table I. Trial runs with about twice the number of water molecules revealed no significant finite-size effects [19, 20] on static properties and orientational dynamics, consistent with a previous study [21] at similar conditions.

When a field $\mathbf{E}_0$ is applied to the system, a term is

$\mathbf{E}$/ V Å^{-1}	0.009	0.015	0.021	0.030	0.040
$\epsilon_m(\mathbf{E})$	65	60	55	48	43

TABLE II: Field $\mathbf{E}$ and associated dielectric constant $\epsilon_m(\mathbf{E})$ (computed as in Ref. [24]).

added to the energy of the system to describe the interaction of the field with partial charges q_i of oxygen and hydrogen atoms in SPC/E water, $U_{field} = \sum_i q_i \mathbf{r}_i \mathbf{E}_0$ where $\mathbf{r}_i$ are the positions of the charges. We have computed the electrostatic interactions with an Ewald sum. To correct for the presence of a depolarizing layer at the surface of the macroscopic system being simulated, we apply the vacuum boundary condition [22], adding a term to the energy $U_{surf} = \frac{2\pi}{3V}|\mathbf{M}|^2$ where $\mathbf{M}$ is the total dipole moment of the system. Consistent with molecule-based (as opposed to atom-based) periodic conditions, the sum $\mathbf{M} = \sum_i q_i \mathbf{r}_i$ comprises partial charges of all water oxygens inside the periodic box, along with adjacent, covalently bound hydrogen atoms. The large dipole moment induced by the electric field warrants the inclusion of this depolarizing term. In this way we mimic an experimental system where a field $\mathbf{E}_0$ is applied in the vacuum/air outside the medium and is screened inside the medium so that $\mathbf{E}$, the actual field in the medium is given by [23]

$$\mathbf{E} = 3\mathbf{E}_0/(\epsilon_m(\mathbf{E}) + 2). \quad (1)$$

Here $\epsilon_m(\mathbf{E})$ is the field dependent dielectric constant of the medium in conducting boundaries computed as in Ref. [24]. From Eqn. 1 and $\epsilon_m(\mathbf{E})$ we can convert between $\mathbf{E}_0$ and $\mathbf{E}$. These data are given in Table II; note that ϵ_m is significantly reduced compared with pure water [25] due to the presence of the nanoparticle. By expressing our findings in terms of the screened field $\mathbf{E}$ we can more easily compare with analytical data [1].

The nanoparticle orients preferentially to be parallel to the electric field. The only nonvanishing component of the torque τ acts around $\mathbf{n} \times \mathbf{E}$, the vector orthogonal to $\mathbf{n}$ (the vector normal to the nanoparticle plane) and $\mathbf{E}$, and so for the rest of the paper we refer only to the absolute (scalar) value of the torque. For small angles ϕ between $\mathbf{E}$ and the plane of the nanoparticle, we can approximate the torque as a linear expansion around $\phi = 0$, $\tau(\phi) = a\phi + O(\phi^2)$ where $a = \lim_{\phi\to 0}(\frac{d\tau}{d\phi})$ and $\tau(0) = 0$ by symmetry. Combining this with the Boltzmann equation we obtain the probability distribution of angles [26],

$$P(\phi) = A\exp(-\frac{a\phi^2}{2k_BT})\cos\phi, \quad (2)$$

where A is a normalization constant. The angle ϕ spans from $-\pi/2$ to $\pi/2$, however the distribution is symmetric around the ideal alignment of $\phi = 0$.

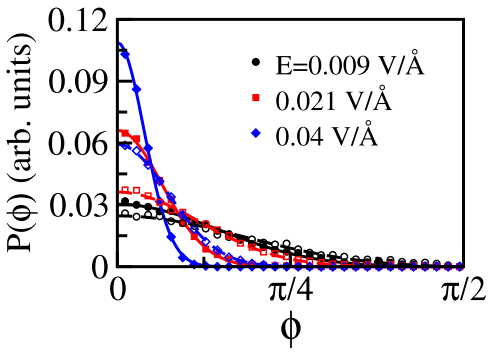

FIG. 1: (Color) Plot of probability distributions for hydrated nanoparticles exposed to electric field. Points are from histograms of the angle ϕ computed in MD simulations, and lines are fits to Equation 2. Solid lines and symbols are for system M1 in Table I), and dashed lines and open symbols are for system S.

As shown in Figure 1, Eqn. 2 provides an excellent description of the simulated angle distributions. In Fig. 2a we compare the value of the fit parameter a obtained from *i*) the fits to Eqn. 2, *ii*) a direct computation of the torque as a function of ϕ, obtained from the MD trajectories, and *iii*) analytical estimates of the torques based on continuum electrostatics [1]. The analytical estimates were computed by describing the nanoparticle as an oblate ellipsoid, with the radii (b_{el} and c_{el} in Table I) chosen to match the moments of inertia of the planar nanoparticle. Imposing additional conditions of equal particle surface areas and volumes (leading to a minor asymmetry between a_{el} and b_{el} and a slight reduction in c_{el}) showed no significant change in calculated torques (below 5%) around either of the two major axes a_{el}, b_{el}. The only net torque acts to rotate the particle around the $\mathbf{n} \times \mathbf{E}$ axis. The solid lines in Figure 2a represent a nonpolar nanoparticle having $\epsilon = 1$ oriented in a water medium with $\epsilon_m(\mathbf{E})$ given by Table II.

Scaling relations from continuum theory enable extrapolations of numerical results to different particle geometries. If the size of the ellipsoid is increased isotropically, the torque scales as b_{el}^3. If only b_{el} is increased, keeping c_{el} fixed, the scaling exponent asymptotically approaches the value 2 for very large b_{el}, but can be greater than 3 for smaller nanoparticles (~ 3.2 for scaling between the small and the large nanoparticle in the current study). This scaling behaviour is close to our simulated results, where $\tau \propto b_{el}^{3.6}$.

The analytical result underestimates the torque by an approximate factor of two. We attribute the difference to an additional orientational effect due to the preference for water molecules to maintain as many hydrogen bonds as possible at the interface [14, 15]. These microscopic effects introduce additional torque, captured by MD but overlooked in continuum models. In fact, a material with $\epsilon \approx \epsilon_m$ (eg. functionalized nanotubes in water), which

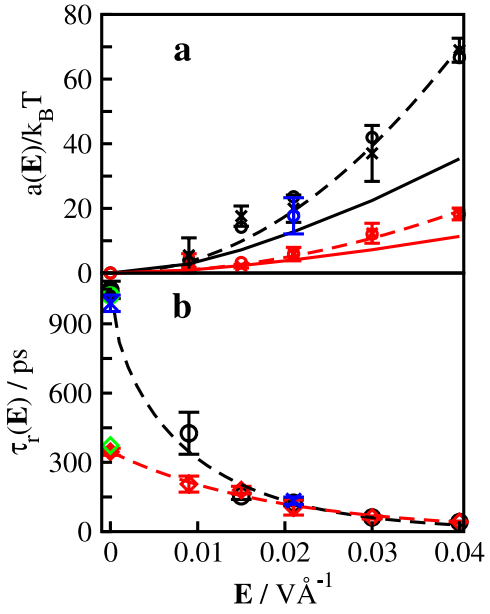

FIG. 2: (Color) Response of the nanoparticle to field **E**. In both plots, black lines/symbols are for system M1 in Table I, blue ones are for system M2, while red ones are for system S. Dashed lines are guides to the eye. Error bars are one standard deviation in the mean, computed from several 5 ns trajectories, except for system M2 where four sets of only ~ 1 ns of data were available. (**a**): Comparison of values of the parameter a in Eqn. 2 from *i*) fits of the probability distributions in Figure 1 to Eqn. 2 (circles), *ii*) direct computation of the torque as a function of ϕ ($\times$'s), and *iii*) from analytical estimates [1] of the torque on a dielectric ellipsoid (solid lines). (**b**): Decay times τ_r from fits of $C_1^\omega(t)$ (solid symbols) and $C_\theta(t)$ (open symbols) to $\exp[-t/\tau_r]$ at short times. Green open symbols are numerical estimates [27] of τ_r for ellipsoidal nanoparticles (see text).

would not be affected by the field according to macroscopic theory, would still experience a torque due to the steric effects on water molecules at the interface. It is this sort of effect we hope may manifest experimentally in order to support our predictions. Other factors which may contribute to the difference include our assumption that a planar nanoparticle can be described as an ellipsoid, and the fact that the dielectric "constant" is anisotropic [17, 28] in highly asymmetric and interfacial systems such as ours [39]. Proper consideration of ϵ_m as a spatially varying tensor might improve the agreement.

How long does it take for these nonpolar nanoparticles to respond to and orient in the electric field? In zero field, the dynamics of a rotating nanoparticle are well quantified in terms of the rotational autocorrelation functions [29],

$$C_1^\omega(t) = \langle P_1[\omega(0)\cdot\omega(t)]\rangle, \qquad (3)$$

where $P_1[x]$ is the first order Legendre polynomial and $\omega(t)$ is a time-varying unit vector along one of the axes of the nanoparticle. We define an axis system where one axis is **n** defined above and the other two axes are along the lattice edges. As time passes, the orientation of the nanoparticle diverges from its initial orientation and $C_1^\omega(t) \to 0$.

When a field is applied, initial states $t = 0$ with different orientations are no longer equivalent. We track the normal angle θ between **n** and **E** (note that above $\phi = \pi/2 - \theta$), and compute a different orientational correlation function,

$$C_\theta(t) = \frac{\langle \cos[\theta(0)]\cdot\cos[\theta(t)]\rangle}{\langle \cos^2\theta\rangle}. \qquad (4)$$

At $t = 0$, $C_\theta(0) = 1$. As time passes, the effect of the electric field tends to return the nanoparticle to a perfect orientation of $\theta = \pi/2$. Thus $C_\theta(t) \to 0$ as t increases.

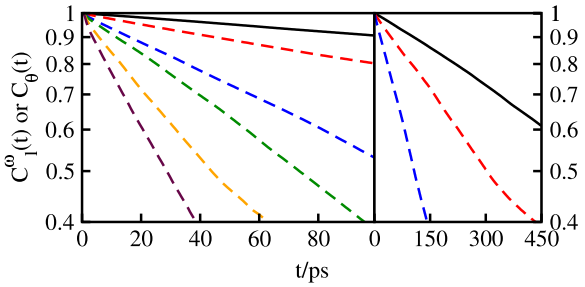

FIG. 3: (Color online) Plots of $C_1^\omega(t)$ (no field, solid line) and $C_\theta(t)$ (dashed lines, at fields **E** given in Table II, with faster decay times as field increases) for the medium nanoparticle (M1). Average of results from several 5 ns trajectories, with data collected every 0.5 ps.

In Figure 3 we show the results of computing $C_1^\omega(t)$ with $\mathbf{E} = 0$ and $C_\theta(t)$ when $\mathbf{E} > 0$. We show $C_1^\omega(t)$ for rotation about **n**; choosing other axes did not show significantly different behavior. Except for the first few ps of $C_\theta(t)$, featuring a faster decay likely due to some ballistic motion between collisions with water molecules (not shown), it is evident that at least at short times ($t \sim 2-100$ ps) both orientational correlation functions follow an exponential decay, ie. $C(t) \sim \exp[-t/\tau_r]$. By fitting a straight line to the semilog plot of the autocorrelation functions over the relevant range (2-100 ps at lower fields, less in larger fields due to statistical noise at longer times) we have computed the decay constants τ_r. We display these results in Figure 2b.

In zero field, the inherent rotational timescales for nanoparticles in systems M1 and M2 are about 1 ns, and about 350 ps for system S. These timescales can also be computed analytically by approximating the planar nanoparticle as an oblate ellipsoid [27, 30]. Using the geometry described in Table I and the value of the shear viscosity $\eta = 6.6 \times 10^{-4}$ Pa s computed for SPC/E water [31], we obtain for the rotational diffusion constant around **n**, $D_r = 4.9 \times 10^8$ s^{-1} for the large nanoparticle and $D_r = 1.3 \times 10^9$ s^{-1} for the small one. Assuming Debye-type relaxation, the relaxation time τ_r of

$C_1^{\omega}(t) = 1/2D_r$ and so we obtain $\tau_r = 1020$ ps for systems M1 and M2 and $\tau_r = 370$ ps for system S, in excellent agreement with our simulated timescales. The analytical estimates of τ_r scale as $\sim b_{el}^{2.8}$, close to our data where $\tau_r \propto b_{el}^{3.1}$. Within statistical error, the $b_{el}^{3.1}$ scaling is confirmed in trial runs for the largest system L in Table I characterized by reorientational time of ~ 3.6 ns. For very large nanoparticles which could be approximated as discs, the scaling exponent asymptotically approaches 3.

As the field strength increases, the timescale for restoration of the parallel nanoparticle orientation shortens, with the decrease more pronounced for larger nanoparticles. In fact, for $\mathbf{E} \geq 0.015$ V/Å the restoration timescales for systems S and M1 are identical within statistical noise as the increased torque on the larger nanoparticle offsets the inherently faster rotation of the smaller nanoparticle. The reorientation time of the nanoparticle in system M1 for field $\mathbf{E} \geq 0.015$ V/Å is an order of magnitude less than its orientational time in the field-free case.

In summary, the torque applied to the nanoparticle exceeds k_BT at experimentally realizable field strengths where electrodes are well-insulated (eg. at the tip of an AFM [32, 33]), so that the effect of the torque is much greater than the effect of thermal fluctuations. The torque we compute from MD is approximately twice stronger than that obtained by continuum electrostatics. In addition, the timescale for reorientation of a nanoparticle decreases dramatically as the field magnitude is increased. For $\mathbf{E} \geq 0.015$ V/Å these timescales are fast (< 250 ps), and for the particles we studied *did not depend on their size*. Both the large torque and the fast dynamics should be of interest as researchers extend nanoengineering methods to smaller length scales[40].

We thank José Teixeira and Kevin Leung for their helpful comments. Support from the National Science Foundation in grants CHE-0718724 (to A.L.) and CBET-0432625 (D.B.) is gratefully acknowledged.

* Corresponding author; Electronic address: aluzar@vcu.edu

[1] J. A. Stratton, *Electromagnetic Theory* (McGraw-Hill, New York, 1941).
[2] H. Y. Hsu *et al.*, Nanotechnology **16**, 312 (2005).
[3] D. Padmaraj *et al.*, Nanotechnology **20**, 035201 (2009).
[4] H. Morgan and N. G. Green, J. Electrostatics **42**, 279 (1997).
[5] N. G. Green and T. B. Jones, J. Phys. D: Appl. Phys. **40**, 78 (2007).
[6] K. D. Hermanson *et al.*, Science **294**, 1082 (2001).
[7] D. L. Fan *et al.*, Appl. Phys. Lett. **89**, 223115 (2006).
[8] J. Park and W. Lu, Appl. Phys. Lett. **91**, 053113 (2007).
[9] J. Park and W. Lu, J. Comput. Theor. Nanosci. **5**, 659 (2008).
[10] X. Zhang, Z. L. Zhang, and S. C. Glotzer, J. Phys. Chem. C **111**, 4132 (2007).
[11] D. Bratko *et al.*, Faraday Discuss. **141**, 55 (2009).
[12] K. Leung, A. Luzar, and D. Bratko, Phys. Rev. Lett. **90**, 065502 (2003).
[13] D. Bratko *et al.*, Phys. Chem. Chem. Phys. **10**, 6807 (2008).
[14] D. Bratko *et al.*, J. Am. Chem. Soc. **129**, 2504 (2007).
[15] C. D. Daub *et al.*, J. Phys. Chem. C **111**, 505 (2007).
[16] S. H. L. Klapp and M. Schoen, J. Chem. Phys. **117**, 8050 (2002).
[17] S. H. L. Klapp and V. A. Froltsov, J. Chem. Phys. **126**, 114703 (2007).
[18] H. J. C. Berendsen *et al.*, J. Phys. Chem. **91**, 6269 (1987).
[19] D. M. Heyes *et al.*, Mol. Phys. **88**, 1503 (1996); J. Phys.: Condens. Matter **46**, 513 (1982).
[20] C. Yeh and G. Hummer, J. Phys. Chem. B **108**, 15873 (2004).
[21] K. Takemura and A. Kitao, J. Phys. Chem. B **111**, 11870 (2007).
[22] S. W. Deleeuw *et al.*, Proc. Roy. Soc. A **373**, 27 (1980).
[23] H. Fröhlich, *Theory of Dielectrics* (Clarendon Press, Oxford, 1958).
[24] G. Sutmann, J. Electroanal. Chem. **450**, 289 (1998).
[25] R. P. Joshi *et al.*, J. Appl. Phys. **96**, 3617 (2004).
[26] J. L. Barrat and J. P. Hansen, *Basic Concepts for Simple and Complex Liquids* (Cambridge University Press, Cambridge, 2003).
[27] J. Lyklema, *Fundamentals of Interface and Colloid Science Volume I: Fundamentals* (Academic Press, London, 1991).
[28] V. Ballenegger and J. P. Hansen, J. Chem. Phys. **122**, 114711 (2005).
[29] R. W. Impey *et al.*, Mol. Phys. **46**, 513 (1982).
[30] J. Perrin, J. Phys. Radium (VII) **5**, 33 (1934).
[31] S. Balasubramanian, C. J. Mundy, and M. L. Klein, J. Chem. Phys. **105**, 11190 (1996).
[32] A. Philippsen *et al.*, Biophys. J. **82**, 1667 (2002).
[33] L. Guan *et al.*, J. Phys. Chem. C **113**, 661 (2009).
[34] S. J. Plimpton, J. Comp. Phys. **117**, 1 (1995).
[35] T. Werder *et al.*, J. Phys. Chem. B **107**, 1345 (2003).
[36] I. C. Yeh and M. L. Berkowitz, J. Chem. Phys. **111**, 3155 (1999).
[37] J. Dzubiella and J.-P. Hansen, J. Chem. Phys. **122**, 234706 (2005).
[38] We used a recent LAMMPS code [34] (updated 21 May 2008), modified to implement the vacuum boundary condition as described in the text. Nosé-Hoover thermostat/barostat maintained the average temperature at 300 K, and atmospheric pressure. The water-nanoparticle potential was the same as that derived in Ref. [35] for a hydrophobic nanoparticle.
[39] We note that the behavior of the current system is essentially different from that of the water slab confined by infinite planar walls [11], where anisotropic screening [36, 37] in directions parallel and perpendicular to the interface leads to larger torque.
[40] For very large planar particles (linear size $\gtrsim 100$ nm) the friction scales with particle size faster than the torque (r^3 vs. r^2), so that larger field strengths would be required to orient larger nanoparticles as quickly.